New Ambipolar Organic Semiconductors. 1. Synthesis, Single-Crystal Structures, Redox Properties, and Photophysics of Phenoxazine-Based Donor−Acceptor Molecules

Yan Zhu, Abhishek P. Kulkarni, Pei-Tzu Wu, and Samson A. Jenekhe*

Departments of Chemical Engineering and of Chemistry, University of Washington, Seattle, Washington 98195

Received August 6, 2007. Revised Manuscript Received April 8, 2008

We report the synthesis and structural, photophysical, and electrochemical properties of a series of eight new phenoxazine-based donor−acceptor molecules utilizing phenoxazine as a common donor and quinoline, quinoxaline, benzoylquinoxaline, and benzoquinoxaline as various electron acceptor moieties. The phenoxazine−phenylquinoline molecules crystallized in the monoclinic system with the space groups $C2/c$ and $P2_1/c$, respectively, revealing a 169° dihedral angle in the phenoxazine unit. The new materials had high glass transition temperatures (128−193 °C) and ambipolar redox properties with reversible electrochemical oxidation and reduction. Their HOMO levels were at 5.1−5.2 eV, whereas their LUMO levels (2.3−3.0 eV) increased with the electron acceptor strength. The materials showed intramolecular charge transfer fluorescence in dilute solutions with emission colors varying from blue to red and a quantum yield ranging from 86% in the phenoxazine−biphenyl molecule to as low as 16% in the benzoquinoxaline-containing molecule. Density functional theory calculations provided insight into the molecular geometry and electronic structures of the donor−acceptor molecules and were in good agreement with the experimental results. These results demonstrate that the new phenoxazine-based donor−acceptor molecules represent a new class of promising ambipolar semiconductors for organic electronics.

Introduction

Multifunctional organic materials with donor−acceptor (D−A) architecture capable of ambipolar charge (electron and hole) injection/transport have recently attracted considerable attention for diverse applications in organic electronics, including organic light-emitting diodes (OLEDs),[1–8] electrogenerated chemiluminescence (ECL),[9,10] photovoltaic cells,[11] and thin film transistors.[12] D−A molecules with bipolar charge transport and high solid-state photoluminescence (PL) quantum yields are especially attractive as

* To whom correspondence should be addressed. E-mail: jenekhe@u.washington.edu.

(1) Reviews on various aspects of organic electroluminescence: (a) Kraft, A.; Grimsdale, A. C.; Holmes, A. B. *Angew. Chem., Int. Ed.* **1998**, *37*, 402. (b) Mitschke, U.; Bäuerle, P. *J. Mater. Chem.* **2000**, *10*, 1471. (c) Heeger, A. J. *Solid State Commun.* **1998**, *107*, 673. (d) Kulkarni, A. P.; Tonzola, C. J.; Babel, A.; Jenekhe, S. A. *Chem. Mater.* **2004**, *16*, 4556. (e) Shirota, Y. *J. Mater. Chem.* **2005**, *15*, 75.

(2) (a) Jenekhe, S. A.; Lu, L.; Alam, M. M. *Macromolecules* **2001**, *34*, 7315. (b) Zhu, Y.; Kulkarni, A. P.; Jenekhe, S. A. *Chem. Mater.* **2005**, *17*, 5225. (c) Kulkarni, A. P.; Wu, P.-T.; Kwon, T. W.; Jenekhe, S. A. *J. Phys. Chem. B* **2005**, *109*, 19584. (d) Kulkarni, A. P.; Kong, X.; Jenekhe, S. A. *Adv. Funct. Mater.* **2006**, *16*, 1057. (e) Hancock, J. M.; Gifford, A. P.; Zhu, Y.; Lou, Y.; Jenekhe, S. A. *Chem. Mater.* **2006**, *18*, 4924. (f) Kulkarni, A. P.; Zhu, Y.; Jenekhe, S. A. *Macromolecules* **2005**, *38*, 1553.

(3) (a) Tamoto, N.; Adachi, C.; Nagai, K. *Chem. Mater.* **1997**, *9*, 1077. (b) Antoniadis, H.; Inbasekaran, M.; Woo, E. P. *Appl. Phys. Lett.* **1998**, *73*, 3055. (c) Shirota, Y.; Kinoshita, M.; Noda, T.; Okumoto, K.; Ohara, T. *J. Am. Chem. Soc.* **2000**, *122*, 11021.

(4) (a) Hamada, Y.; Adachi, C.; Tsutsui, T.; Saito, S. *Jpn. J. Appl. Phys.* **1992**, *31*, 1812. (b) Goes, M.; Verhoeven, J. W.; Hofstraat, H.; Brunner, K. *ChemPhysChem* **2003**, *4*, 349. (c) Tao, Y.-T.; Chuen, C.-H.; Ko, C. W.; Peng, J. W. *Chem. Mater.* **2002**, *14*, 4256. (d) Zhu, Y.; Gibbons, K. M.; Kulkarni, A. P.; Jenekhe, S. A. *Macromolecules* **2007**, *40*, 804.

(5) (a) Thomas, K. R. J.; Lin, J. T.; Tao, Y.-T.; Chuen, C.-H. *Chem. Mater.* **2002**, *14*, 3852. (b) Zhu, W.; Hu, M.; Yao, R.; Tian, H. *J. Photochem. Photobiol. A* **2003**, *154*, 169.

(6) (a) Kelnhofer, K.; Knorr, A.; Tak, Y.-H.; Bässler, H.; Daub, J. *Acta Polym.* **1997**, *48*, 188. (b) Thomas, K. R. J.; Lin, J. T.; Tao, Y.-T.; Chuen, C.-H. *J. Mater. Chem.* **2002**, *12*, 3516.

(7) (a) Thomas, K. R. J.; Lin, J. T.; Velusamy, M.; Tao, Y.-T.; Chuen, C.-H. *Adv. Funct. Mater.* **2004**, *14*, 83. (b) Chiang, C.-L.; Wu, M.-F.; Dai, D.-C.; Wen, Y.-S.; Wang, J.-K.; Chen, C.-T. *Adv. Funct. Mater.* **2005**, *15*, 231. (c) Sun, X.; Liu, Y.; Xu, X.; Yang, C.; Yu, G.; Chen, S.; Zhao, Z.; Qiu, W.; Li, Y.; Zhu, D. *J. Phys. Chem. B* **2005**, *109*, 10786.

(8) (a) Brunner, K.; van Dijken, A.; Börner, H.; Bastiaansen, J. J. A. M.; Kiggen, N. M. M.; Langeveld, B. M. W. *J. Am. Chem. Soc.* **2004**, *126*, 6035. (b) Thomas, K. R. J.; Lin, J. T.; Tao, Y.-T.; Ko, C.-W. *J. Am. Chem. Soc.* **2001**, *123*, 9404. (c) Morin, J.-F.; Drolet, N.; Tao, Y.; Leclerc, M. *Chem. Mater.* **2004**, *16*, 4619.

(9) (a) Richter, M. M. *Chem. Rev.* **2004**, *104*, 3003. (b) Armstrong, N. R.; Wightman, R. M.; Gross, E. M. *Annu. Rev. Phys. Chem.* **2001**, *52*, 391. (c) Dini, D. *Chem. Mater.* **2005**, *17*, 1933.

(10) (a) Richter, M. M.; Fan, F. F.; Klavetter, F.; Heeger, A. J.; Bard, A. J. *Chem. Phys. Lett.* **1994**, *226*, 115. (b) Anderson, J. D.; McDonald, E. M.; Lee, P. A.; Anderson, M. L.; Ritchie, E. L.; May, H. K.; Hopkins, T.; Mash, E. A.; Wang, J.; Padias, A.; Thayumanavan, S.; Barlow, S.; Marder, S. R.; Jabbour, G. E.; Shaheen, S.; Kippelen, B.; Peyghambarian, N.; Wightman, R. M.; Armstrong, N. R. *J. Am. Chem. Soc.* **1998**, *120*, 9646. (c) Pei, Q.; Yang, Y.; Yu, G.; Heeger, A. J. *J. Am. Chem. Soc.* **1996**, *118*, 3922. (d) Lai, R. Y.; Fabrizio, E. F.; Lu, L.; Jenekhe, S. A.; Bard, A. J. *J. Am. Chem. Soc.* **2001**, *123*, 9112. (e) Lai, R. Y.; Kong, X.; Jenekhe, S. A.; Bard, A. J. *J. Am. Chem. Soc.* **2003**, *125*, 12631. (f) Knorr, A.; Daub, J. *Angew. Chem., Int. Ed. Engl.* **1995**, *34*, 2664. (g) Ketter, J. B.; Wightman, R. M. *J. Am. Chem. Soc.* **2004**, *126*, 10183.

(11) (a) Jenekhe, S. A.; Yi, S. *Appl. Phys. Lett.* **2000**, *77*, 2635. (b) Alam, M. M.; Jenekhe, S. A. *J. Phys. Chem. B* **2001**, *105*, 2479. (c) Alam, M. M.; Jenekhe, S. A. *Chem. Mater.* **2004**, *16*, 4647. (d) Yu, G.; Gao, J.; Hummelen, J. C.; Wudl, F.; Heeger, A. J. *Science* **1995**, *270*, 1789. (e) Sonmez, G.; Shen, C. K. F.; Rubin, Y.; Wudl, F. *Adv. Mater.* **2005**, *17*, 897. (f) Svensson, M.; Zhang, F.; Veenstra, S. C.; Verhees, W. J. H.; Hummelen, J. C.; Kroon, J. M.; Inganäs, O.; Andersson, M. R. *Adv. Mater.* **2003**, *15*, 988. (g) Wider, C.; Sariciftci, N. S. *J. Mater. Chem.* **2004**, *14*, 1077.

10.1021/cm702212w CCC: $40.75
Published on Web 06/04/2008

efficient emitters for the development of high-performance OLEDs.[1–8] The electroluminescence (EL) from D−A molecules can originate from intramolecular charge transfer (ICT) excited states formed by the annihilation reaction between the donor radical cations and the acceptor radical anions.[2,4b,6] Thus, a highly desired feature of such emissive materials is to have proper energy levels that are matched to electrodes for charge carrier injection of both holes and electrons; further, they should form very stable radical cations and radical anions, a requirement that is very similar to that for ECL.[9,10] A judicious choice of the donor and acceptor moieties could facilitate simultaneous manipulation of the HOMO/LUMO energy levels, the emission color, and other physical properties of the D−A molecules.

Numerous emissive D−A molecules have been reported, and EL colors spanning the whole visible region, including blue,[4] green,[2b–e,3c,5] yellow,[5a,6] and red,[7] have been achieved from OLEDs based on these materials. Systematic studies of the structure−property relationships of D−A molecules are essential for the design of next-generation ambipolar emissive materials for OLEDs. Oxadiazole,[3a,b,4a,5a] diarylboron,[3c] benzothiadiazole,[7a] and quinoxaline[2e,6b] are commonly used electron acceptor moieties in D−A molecules. Triarylamine,[3,4a,c,7a,c] carbazole,[6b,8] and fluorene[3b] and their derivatives have been extensively studied as electron donors in hole transport or emissive materials for OLEDs. Phenoxazine and phenothiazine, which have a fused tricyclic structure similar to that of carbazole, are stronger and potentially better electron donors than the carbazole unit due to their 0.7 eV lower ionization potentials and thus more stable radical cations.[2a–d,13] In contrast to the vast literature on carbazole-containing emissive molecules,[6b,8] phenothiazine and phenoxazine are scarcely explored as building blocks in current OLED materials. There are only a few previous reports of OLEDs based on phenothiazine-containing materials,[2c,d,6a,7c] although phenothiazine has been extensively investigated as a donor in ECL systems.[6a,9a,10d–f] Compared to phenothiazine, phenoxazine has attracted even much less attention as a building block in organic semiconductors.[14] Several 1,4-benzoxazino[2,3-*b*]phenoxazines have been prepared and used as hole injection materials in OLEDs.[14b] A random copolymer of phenoxazine and fluorene was employed as an emissive layer in OLEDs very recently.[14c] However, phenoxazine-based donor−acceptor molecules have not yet been studied and explored as emissive materials for OLEDs except in our preliminary work.[2b] In that paper, we reported the synthesis and preliminary fabrication of bright and efficient green OLEDs from two fluorescent phenoxazine−phenylquinoline donor−acceptor molecules.[2b]

In this paper, we report the synthesis, detailed structural characterization, and investigation of the electrochemical and photophysical properties of a series of eight new donor−acceptor molecules incorporating phenoxazine as a common donor and various n-type moieties, including quinoline, quinoxaline, benzoquinoxaline, and benzoylquinoxaline, as the acceptors with the aim to develop a clear understanding of structure−property relationships in the D−A molecules relevant to solid-state electronic devices. The molecular structures of the phenoxazine molecules 3,7-bis(biphenyl-4-yl)-10-hexyl-10*H*-phenoxazine (BP-HPO, **1**), 3,7-bis(4-phenylquinolin-2-yl)-10-phenyl-10*H*-phenoxazine (PQ-PPO, **2**), 3,7-bis(4-phenylquinolin-2-yl)-10-methyl-10*H*-phenoxazine (PQ-MPO, **3**), 3,7-bis(4-methylquinolin-2-yl)-10-phenyl-10*H*-phenoxazine (MQ-PPO, **4**), 3,7-bis(4-methylquinolin-2-yl)-10-methyl-10*H*-phenoxazine (MQ-MPO, **5**), 3,7-bis(3-phenylquinoxalin-2-yl)-10-phenyl-10*H*-phenoxazine (PQx-PPO, **9**), 3,7-bis(3-phenylbenzo[*g*]quinoxalin-2-yl)-10-phenyl-10*H*-phenoxazine (BQx-PPO, **10**), and {3-[7-(7-benzoyl-3-phenylquinoxalin-2-yl)-10-phenyl-10*H*-phenoxazin-3-yl]-2-phenylquinoxalin-6-yl}phenylmethanone (BzQx-PPO, **11**) are shown in Chart 1. Quinoxaline moieties were chosen as acceptor building blocks because quinoxaline-containing small molecules and polymers have been widely used as electron transport and emissive materials for OLEDs.[2e,6b,15] Although oligoquinolines[16] and polyquinolines[1d,17] have been demonstrated as good electron transport materials in OLEDs, the quinoline moiety has only recently been incorporated into D−A molecules for OLEDs.[2b–e] The effects of the electron acceptor structure and strength on the molecular conformation and geometry, redox properties, HOMO/LUMO energy levels, and charge transfer photophysics of the phenoxazine-based D−A molecules were fully investigated.

Experimental Section

Materials. All commercially available reagents were purchased from Aldrich and used without further purification. 3,7-Dibromo-10-hexylphenoxazine,[14a] 3,7-diacetyl-10-phenylphenoxazine,[2b] 3,7-diacetyl-10-methylphenoxazine,[2b] and 10-phenylphenoxazine[2b] were prepared according to the literature methods.

3,7-Bis(biphenyl-4-yl)-10-hexyl-10*H*-phenoxazine (BP-HPO, 1). To a three-necked flask were added 3,7-dibromo-10-hexylphenoxazine (600 mg, 1.4 mmol), 4-biphenylboronic acid (614 mg,

(12) (a) Champion, R. D.; Cheng, K.-F.; Pai, C.-L.; Chen, W.-C.; Jenekhe, S. A. *Macromol. Rapid Commun.* **2005**, *26*, 1835. (b) Babel, A.; Wind, J. D.; Jenekhe, S. A. *Adv. Funct. Mater.* **2004**, *14*, 891. (c) Yamamoto, T.; Yasuda, T.; Sakai, Y.; Aramaki, S. *Macromol. Rapid Commun.* **2005**, *26*, 1214. (d) Chen, M.; Crispin, X.; Perzon, E.; Andersson, M. R.; Pullerits, T.; Andersson, M.; Inganäs, O.; Berggren, M. *Appl. Phys. Lett.* **2005**, *87*, No. 252105.

(13) (a) Bloor, J. E.; Gilson, B. R.; Haas, R. J.; Zirkle, C. L. *J. Med. Chem.* **1970**, *13*, 922. (b) Bressler, D. C.; Fedorak, P. M.; Pickard, M. A. *Biotechnol. Lett.* **2000**, *22*, 1119.

(14) (a) Zhu, Y.; Babel, A.; Jenekhe, S. A. *Macromolecules* **2005**, *38*, 7983. (b) Okamoto, T.; Kozaki, M.; Doe, M.; Uchida, M.; Wang, G.; Okada, K. *Chem. Mater.* **2005**, *17*, 5504. (c) Ito, Y.; Shimada, T.; Ha, J.; Vacha, M.; Sato, H. *J. Polym. Sci., Part A: Polym. Chem.* **2006**, *44*, 4338.

(15) (a) Cui, Y.; Zhang, X.; Jenekhe, S. A. *Macromolecules* **1999**, *32*, 3824–3826. (b) Yamamoto, T.; Sugiyama, K.; Kushida, T.; Inoue, T.; Kanbara, T. *J. Am. Chem. Soc.* **1996**, *118*, 3930. (c) O'Brien, D.; Weaver, M. S.; Lidzey, D. G.; Bradley, D. D. C. *Appl. Phys. Lett.* **1996**, *69*, 881. (d) Jandke, M.; Strohriegl, P.; Berleb, S.; Werner, E.; Brütting, W. *Macromolecules* **1998**, *31*, 6434.

(16) (a) Kulkarni, A. P.; Gifford, A. P.; Tonzola, C. J.; Jenekhe, S. A. *Appl. Phys. Lett.* **2005**, *86*, 061106. (b) Tonzola, C. J.; Kulkarni, A. P.; Gifford, A. P.; Kaminsky, W.; Jenekhe, S. A. *Adv. Funct. Mater.* **2007**, *17*, 863. (c) Hancock, J. M.; Gifford, A. P.; Tonzola, C. J.; Jenekhe, S. A. *J. Phys. Chem. C* **2007**, *111*, 6875.

(17) (a) Zhang, X.; Shetty, A. S.; Jenekhe, S. A. *Macromolecules* **1999**, *32*, 7422. (b) Zhang, X.; Jenekhe, S. A. *Macromolecules* **2000**, *33*, 2069. (c) Zhu, Y.; Alam, M. M.; Jenekhe, S. A. *Macromolecules* **2003**, *36*, 8958. (d) Tonzola, C. J.; Alam, M. M.; Jenekhe, S. A. *Adv. Mater.* **2002**, *14*, 1086. (e) Tonzola, C. J.; Alam, M. M.; Jenekhe, S. A. *Macromolecules* **2005**, *38*, 9539. (f) Jenekhe, S. A.; Zhang, X.; Chen, X. L.; Choong, V.-E.; Gao, Y.; Hsieh, B. R. *Chem. Mater.* **1997**, *9*, 409. (g) Jenekhe, S. A.; Alam, M. M.; Zhu, Y.; Jiang, S. Y.; Shevade, A. V. *Adv. Mater.* **2007**, *19*, 536.

Chart 1

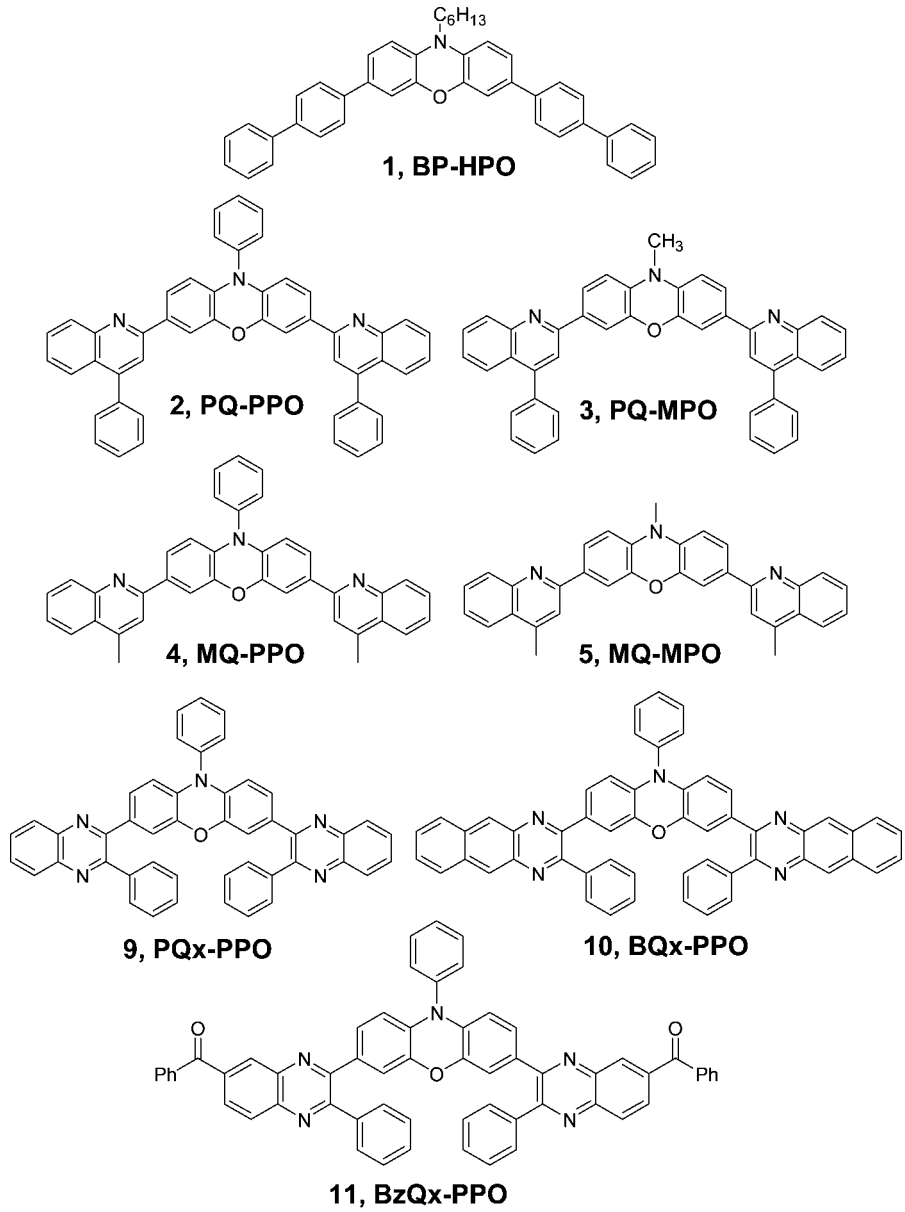

3.1 mol), Aliquat 336 (110.4 mg), and toluene (25 mL). Once all the compounds were dissolved, 2 M aqueous sodium carbonate solution (17 mL) was added. The flask equipped with a condenser was then evacuated and filled with argon several times to remove traces of air. $Pd(PPh_3)_4$ (33 mg, 0.03 mmol) was then added under an argon atmosphere. The mixture was then stirred for 24 h at 110 °C under argon. After the mixture was cooled to room temperature, the yellow precipitate was filtered out, washed with water and ethanol, and dried. The crude product was purified by recrystallization from methylene chloride/methanol to afford compound **1** as light-yellow needles. Yield: 64%. Mp: 276.2−276.9 °C. ^{1}H NMR (300 MHz, CD_2Cl_2): δ 7.68 (m, 12H), 7.50 (t, 4H), 7.39 (t, 2H), 7.20 (d, 2H), 7.04 (s, 2H), 6.67 (d, 2H), 3.62 (t, 2H), 1.78 (m, 2H), 1.44 (m, 6H), 0.98 (t, 3H). FT-IR (KBr pellet, cm^{-1}): 3032, 2928, 2855, 1632, 1593, 1531, 1504, 1483, 1389, 1305, 1277, 1206, 1158, 871, 839, 805, 763, 724, 692. MS (ESI mode) (*m*/*z*): found (M) 571.5; $C_{42}H_{37}NO$ requires (M) 571.75.

3,7-Bis(4-phenylquinolin-2-yl)-10-phenyl-10*H*-phenoxazine (PQ-PPO, 2). 2-Aminobenzophenone (1.38 g, 7.00 mmol) and 3,7-diacetyl-10-phenylphenoxazine (1.00 g, 2.92 mmol) were added along with 9 g of diphenyl phosphate (DPP) and 6 g of *m*-cresol to a flask. The reaction mixture was purged with argon for 20 min, and then the temperature was gradually raised to 90 °C for 1 h and then to 140 °C for 16 h under an argon atmosphere. After cooling, the product was precipitated in a solution of 360 mL of methanol/40 mL of triethylamine. The yellow powder was extracted with a 10% triethylamine/methanol solution for 2 days. Recrystallization from benzene gave **2** as yellow plates (87%). ^{1}H NMR (300 MHz, $CDCl_3$): δ 8.22 (d, 2H), 7.89 (d, 2H), 7.66−7.75 (m, 8H), 7.43−7.58 (m, 17H), 6.09 (d, 2H). FT-IR (KBr pellet, cm^{-1}): 3059, 1588, 1544, 1505, 1429, 1357, 1289, 1131, 1072, 1024, 876, 838, 812, 768, 700, 619. MS (ESI mode) (*m*/*z*): found (M + 1) 666.5; $C_{48}H_{31}N_3O$ requires (M) 665.25. A melting point was not observed in differential scanning calorimetry (DSC) scans up to 370 °C.

3,7-Bis(4-phenylquinolin-2-yl)-10-methyl-10*H*-phenoxazine (PQ-MPO, 3). This compound was prepared by a procedure similar to that of **2** except that 3,7-diacetyl-10-methylphenoxazine was used as the reactant instead of 3,7-diacetyl-10-phenylphenoxazine. The product was purified by column chromatography (silica gel, 2% ethyl acetate/CH_2Cl_2), followed by recrystallization from benzene to afford **3** as an orange powder. Yield: 79%. Mp: 310.9−311.8 °C. ^{1}H NMR (300 MHz, $CDCl_3$): δ 8.23 (d, 2H), 7.90 (d, 2H),

7.70−7.79 (m, 8H), 7.43−7.58 (m, 12H), 6.70 (d, 2H), 3.22 (s, 3H). FT-IR (KBr pellet, cm^{-1}): 3057, 2925, 1632, 1589, 1540, 1511, 1456, 1371, 1293, 1242, 1152, 1113, 857, 804, 765, 700, 577. MS (ESI mode) (*m*/*z*): found (M + 1) 604.5; $C_{43}H_{29}N_3O$ requires (M) 603.23.

3,7-Bis(4-methyl-quinolin-2-yl)-10-phenyl-10*H*-phenoxazine (MQ-PPO, 4). This compound was prepared by a procedure similar to that of **2** except that 2-aminoacetophenone was used as the reactant instead of 2-aminobenzophenone. The product was purified by column chromatography (silica gel, 2% ethyl acetate/CH_2Cl_2) to afford **4** as a yellow powder. Yield: 57%. Mp: 311.6−312.5 °C. ^{1}H NMR (300 MHz, $CDCl_3$): δ 8.17 (d, 2H), 7.98 (d, 2H), 7.44−7.75 (m, 15H), 6.11 (d, 2H), 2.77 (s, 6H). FT-IR (KBr pellet, cm^{-1}): 3058, 1592, 1550, 1501, 1460, 1353, 1332, 1286, 887, 857, 841, 821, 807, 757, 719, 701. MS (ESI mode) (*m*/*z*): found (M) 542.4; $C_{38}H_{27}N_3O$ requires (M) 541.64.

3,7-Bis(4-methylquinolin-2-yl)-10-methyl-10*H*-phenoxazine (MQ-MPO, 5). This compound was prepared by a procedure similar to that of **3** except that 2-aminoacetophenone was used as the reactant instead of 2-aminobenzophenone. The product was purified by column chromatography (silica gel, 2% ethyl acetate/CH_2Cl_2) to afford **5** as a yellow powder. Yield: 50%. Mp: 310.7−311.5 °C. ^{1}H NMR (300 MHz, $CDCl_3$): δ 8.18 (d, 2H), 8.00 (d, 2H), 7.51−7.78 (m, 10H), 6.70 (d, 2H), 3.22 (s, 3H), 2.78 (s, 6H). FT-IR (KBr pellet, cm^{-1}): 3059, 2967, 1634, 1593, 1568, 1551, 1503, 1458, 1430, 1372, 1326, 1283, 1223, 1167, 1118, 894, 856, 839, 799, 770, 753, 721. MS (ESI mode) (*m*/*z*): found (M) 480.3; $C_{33}H_{25}N_3O$ requires (M) 479.57.

3,7-Dibromo-10-phenyl-10*H*-phenoxazine (6). A 400 mg (1.54 mmol) portion of 10-phenylphenoxazine was dissolved in a mixture of chloroform and glacial acetic acid (50 mL/50 mL), and then *N*-bromosuccinimide (NBS) (563 mg, 3.16 mmol) was added to the solution slowly over 20 min. The solution was stirred in the dark for 2 h at room temperature. The solvent was removed under reduced pressure. The residue was dissolved in CH_2Cl_2, washed with brine and water, and dried over sodium sulfate. After the solvent was removed by rotary evaporation, the crude product was purified by column chromatography on silica gel with hexane as the eluent to yield compound **6** (597 mg, 93%) as white crystals. ^{1}H NMR (300 MHz, $CDCl_3$): δ 7.62 (t, 2H), 7.51 (t, 1H), 7.31 (d, 2H), 6.83 (s, 2H), 6.71 (d, 2H), 5.77 (d, 2H). GC−MS showed the presence of only one component with *m*/*z* 417.

10-Phenyl-3,7-bis(phenylethynyl)-10*H*-phenoxazine (7). To a solution of **6** (500 mg, 1.2 mmol) in dry tetrahydrofuran (THF) (20 mL) and triethylamine (20 mL) were added $Pd(PhCN)_2Cl_2$ (27.6 mg, 0.072 mmol), CuI (13.7 mg, 0.072 mmol), and tri-*tert*-butylphosphine (14.6 mg, 0.072 mmol) under argon. Phenylacetylene (343 mg, 3.4 mmol) was then added to the mixture dropwise. The reaction mixture was stirred for 16 h at 60 °C. After the mixture was cooled to room temperature, the solvent was removed under reduced pressure. The resulting residue was dissolved in methylene chloride, washed with water, and dried over anhydrous sodium sulfate. After removal of the solvent, the product was purified by column chromatography on silica gel (70% ether in hexane) to afford compound **7** as a yellow solid. Yield: 65%. ^{1}H NMR (300 MHz, $CDCl_3$): δ 7.65 (t, 2H), 7.49−7.56 (m, 5H), 7.33−7.38 (m, 8H), 6.88 (s, 2H), 6.80 (d, 2H), 5.88 (d, 2H). MS (ESI mode) (*m*/*z*): found (M) 459.3; $C_{34}H_{21}NO$ requires (M) 459.54.

1-[7-(2-Oxo-2-phenylacetyl)-10-phenyl-10*H*-phenoxazin-3-yl]-2-phenylethane-1,2-dione (8). To a solution of **7** (1 g, 2.18 mmol) in DMSO (30 mL) was added I_2 (552 mg, 2.18 mmol). The reaction mixture was stirred at 150 °C for 16 h. It was then poured into a 1% $Na_2S_2O_3$ aqueous solution, and the product was extracted with ether. The combined extracts were washed with water and dried over sodium sulfate. After removal of the solvent, the product was purified by Soxhlet extraction with ethanol followed by column chromatography on silica gel with ether as the eluent to give 798 mg of compound **8** as a yellow solid. Yield: 70%. ^{1}H NMR (300 MHz, $CDCl_3$): δ 7.95 (d, 4H), 7.51−7.67 (m, 9H), 7.23−7.34 (m, 6H), 5.96 (d, 2H). MS (ESI mode) (*m*/*z*): found (M) 524.2; $C_{34}H_{21}NO_5$ requires (M) 523.53.

3,7-Bis(3-phenylquinoxalin-2-yl)-10-phenyl-10*H*-phenoxazine (PQx-PPO, 9). A mixture of compound **8** (1 g, 1.91 mmol) and 1,2-phenylenediamine (413 mg, 3.82 mmol) in ethanol (300 mL) was refluxed for 24 h under argon. After cooling of the reaction to room temperature, the light-yellow precipitate was filtered out, washed with ethanol, and dried. The crude product was purified by Soxhlet extraction with ethanol for 24 h. Yield: 1.06 g, 83%. ^{1}H NMR (300 MHz, CD_2Cl_2): δ 8.12 (d, 4H), 7.79 (d, 4H), 7.40−7.81 (m, 15H), 6.97 (s, 2H), 6.76 (d, 2H), 5.87 (d, 2H). FT-IR (KBr pellet, cm^{-1}): 3061, 1593, 1505, 1420, 1392, 1356, 1285, 1217, 1123, 1060, 929, 876, 819, 805, 761, 697. MS (FAB) (*m*/*z*): found (M) 667.2; $C_{46}H_{29}N_5O$ requires (M) 667.76. A melting point was not observed in DSC scans up to 350 °C.

3,7-Bis(3-phenylbenzo[*g*]quinoxalin-2-yl)-10-phenyl-10*H*-phenoxazine (BQx-PPO, 10). This compound was prepared by a procedure similar to that of **9** except that 2,3-diaminonaphthalene was used as the reactant instead of 1,2-phenylenediamine. Yield: 63%. ^{1}H NMR (300 MHz, $CDCl_3$): δ 8.72 (s, 4H), 8.12 (d, 4H), 7.48−7.69 (m, 17H), 7.34 (d, 2H), 7.07 (s, 2H), 6.77 (d, 2H), 5.86 (d, 2H). FT-IR (KBr pellet, cm^{-1}): 3054, 1591, 1503, 1419, 1350, 1286, 1175, 1126, 1055, 1003, 924, 881, 816, 803, 745, 696, 604. MS (FAB) (*m*/*z*): found (M) 768.3; $C_{54}H_{33}N_5O$ requires (M) 767.87. A melting point was not observed in DSC scans up to 350 °C.

{3-[7-(7-Benzoyl-3-phenylquinoxalin-2-yl)-10-phenyl-10*H*-phenoxazin-3-yl]-2-phenylquinoxalin-6-yl}phenylmethanone (BzQx-PPO, 11). This compound was prepared by a procedure similar to that of **9** except that 3,4-diaminobenzophenone was used as the reactant instead of 1,2-phenylenediamine. The reaction mixture was refluxed for 48 h instead of 24 h to get complete quinoxaline ring cyclization. Yield: 47%. ^{1}H NMR (300 MHz, CD_2Cl_2): δ 8.47 (s, 2H), 8.23 (d, 4H), 7.92 (d, 4H), 7.40−7.65 (m, 21H), 7.00 (s, 2H), 6.79 (d, 2H), 5.88 (d, 2H). FT-IR (KBr pellet, cm^{-1}): 3060, 1660, 1594, 1503, 1448, 1425, 1397, 1350, 1304, 1207, 1179, 1123, 1059, 1027, 1002, 881, 845, 769, 697. MS (FAB) (*m*/*z*): found (M) 876.1; $C_{60}H_{37}N_5O_3$ requires (M) 875.97. A melting point was not observed in DSC scans up to 350 °C.

Characterization. FT-IR spectra were taken on a Perkin-Elmer 1720 FTIR spectrophotometer with KBr pellets. ^{1}H NMR spectra were recorded on a Bruker-AV300 spectrometer at 300 MHz. MS spectra were obtained on a Hewlett-Packard 5971 gas chromatograph−mass spectometer or Bruker Esquire LC/ion trap mass spectrometer. Melting points were determined on an Electrothermal IA9100 digital melting point instrument at a heating rate of 1 °C/min. DSC analysis was performed on a TA Instruments Q100 under N_2 at a heating rate of 10 °C/min. Thermogravimetric analysis (TGA) analysis was conducted with a TA Instruments Q50 at a heating rate of 20 °C/min under a nitrogen gas flow.

Cyclic voltammetry experiments were done on an EG&G Princeton Applied Research potentiostat/galvanostat (model 273A). Data were collected and analyzed by the model 270 electrochemical analysis system software on a PC computer. A three-electrode cell was used in all experiments. Platinum wire electrodes were used as both counter and working electrodes, and silver/silver ion (Ag in 0.1 M $AgNO_3$ solution, Bioanalytical System, Inc.) was used as a reference electrode. The Ag/Ag^+ ($AgNO_3$) reference electrode was calibrated at the beginning of the experiments by running cyclic voltammetry on ferrocene as the internal standard. The potential

values obtained in reference to the Ag/Ag^+ electrode were then converted to the saturated calomel electrode (SCE) scale. Solution cyclic voltammetry was carried out in a 1 mM solution of the compound in a mixed benzene/acetonitrile (2:1, v/v) solvent containing $TBAPF_6$ (0.1 M) as an electrolyte. All solutions were purged with high-purity N_2 for 15−20 min before each experiment, and a blanket of N_2 was used during the experiment.

UV−vis absorption spectra were recorded on a Perkin-Elmer model Lambda 900 UV/vis/near-IR spectrophotometer. The PL emission spectra were obtained with a Photon Technology International (PTI) Inc. model QM-2001-4 spectrofluorimeter. The PL quantum yields of the D−A molecules in dilute (5×10^{-6} M) toluene solution were measured by using a 10^{-5} M solution of perylene in toluene as a standard ($\phi_{PL} = 94\%$).[18] All solutions were degassed with nitrogen for at least 15−20 min before spectral acquisition.

Theoretical Methods. All calculations on the D−A molecules and their parent donor and acceptor units were done with the Gaussian03 program package[19] by using density functional theory (DFT): Becke's three-parameter functional[20] combined with Lee, Yang, and Parr's correlation functional[21] (B3LYP), along with the 6-31G* basis set, was used. Geometry optimizations attempt to locate the minima on the potential energy surface to predict equilibrium structures of a given molecule. Before optimization of ground-state geometries by B3LYP/6-31G* was performed, the molecular structures were initially optimized in semiempirical AM1[22] calculation as recommended in the Gaussian03 program package.

Results and Discussion

Synthesis and Characterization. The synthetic routes to the eight phenoxazine-based D−A molecules are outlined in Scheme 1. The compound BP-HPO (**1**) was synthesized by Suzuki coupling reaction in good yield (64%). The four phenoxazine−quinoline D−A molecules PQ-PPO (**2**), PQ-MPO (**3**), MQ-PPO (**4**), and MQ-MPO (**5**) were synthesized by acid-catalyzed Friedlander condensation[2b,e,17c–e] in moderate to high yield (50−87%). The DPP catalyst was readily removed by precipitation into a 10% triethylamine/methanol solution. The bromination of 10-phenyl-10*H*-phenoxazine with NBS in a mixture of chloroform and glacial acetic acid gave the desired **6** with a high yield (93%). We found that the use of Br_2 instead of NBS as the bromination reagent for 10-phenyl-10*H*-phenoxazine easily gave a mixture of monobromo-, dibromo-, and tribromo-substituted products which were difficult to isolate. A similar observation was also previously reported in the bromination of the related 10-phenyl-10*H*-phenothiazine with bromine.[23] NBS has been shown to be a more efficient bromination reagent for 10-phenyl-substituted phenoxazine or phenothiazine with much higher selectivity and yield compared to bromine. The Sonogashira palladium-catalyzed coupling reaction of compound **6** with phenylacetylene followed by the oxidation of the alkynylated phenoxazine **7** with DMSO and iodine gave rise to **8**. The preparation of phenoxazine−quinoxaline-type D−A molecules PQx-PPO (**9**), BQx-PPO (**10**), and BzQx-PPO (**11**) was achieved by a typical quinoxaline ring-forming reaction, the condensation between an *o*-diamine function and a 1,2-dicarbonyl group,[2e,f,15a] which in the present study involves the condensation of compound **8** with various *o*-diamines. A longer reaction time (48 h) was required to get the complete cyclization in BzQx-PPO compared to the 24 h used in the synthesis of PQx-PPO and BQx-PPO.

^1H NMR spectra, FT-IR spectra, and mass spectra of the D−A molecules and X-ray single-crystal determination on two of them confirmed the proposed structures. All the phenoxazine-based molecules are soluble in organic solvents, such as CH_2Cl_2, tetrahydrofuran, and toluene.

The thermal properties of the new phenoxazine compounds were evaluated by TGA and DSC, and the results are summarized in Table 1. The second heating DSC scans of the D−A molecules are shown in Figure 1. PQ-MPO had a glass transition (T_g) at 137 °C, a 197 °C crystallization peak (T_c), and a melting transition (T_m) at 311 °C. The thermal transitions T_g, T_c, and T_m are 128, 212, and 312 °C, respectively, for MQ-PPO. PQ-PPO showed a glass transition at 149 °C and no melting transition up to 350 °C, whereas MQ-MPO had a melting endotherm at 311 °C but did not exhibit a glass transition up to T_m. As shown in Figure 1B, BP-HPO exhibited a melting endotherm at 276 °C whereas a glass transition and crystallization exotherm were not observed. The three phenoxazine−quinoxaline D−A molecules showed only glass transitions ranging from 154 °C in PQx-PPO to 193 °C in BQx-PPO, and no melting and crystallization events were seen. The increase in the glass transition temperature from PQx-PPO to BzQx-PPO to BQx-PPO is clearly due to the progressive increase of the molecular size. The more rigid structure and bulkier size of the benzoquinoxaline moiety compared to the quinoxaline and benzoylquinoxaline units explain the highest T_g shown by BQx-PPO among the three molecules. The high glass transition temperatures (128−193 °C) observed for the phenoxazine-based molecules suggest robust thermal stability of their amorphous thin films, a desired feature of OLED materials because of the inevitable joule heating under device operating conditions. The onset decomposition temperatures of all the compounds determined by TGA were in the range of 375−501 °C (Table 1), further demonstrating the good thermal stability of the materials.

X-ray Crystal Structures. Single crystals of PQ-PPO and PQ-MPO suitable for the determination of X-ray crystal

(18) Heinrich, G.; Schoof, S.; Gusten, H. *J. Photochem.* **1974**, *3*, 315.
(19) Frisch, M. J.; Trucks, G. W.; Schlegel, H. B.; Scuseria, G. E.; Robb, M. A.; Cheeseman, J. R.; Montgomery, J. A., Jr.; Vreven, T.; Kudin, K. N.; Burant, J. C.; Millam, J. M.; Iyengar, S. S.; Tomasi, J.; Barone, V.; Mennucci, B.; Cossi, M.; Scalmani, G.; Rega, N.; Petersson, G. A.; Nakatsuji, H.; Hada, M.; Ehara, M.; Toyota, K.; Fukuda, R.; Hasegawa, J.; Ishida, M.; Nakajima, T.; Honda, Y.; Kitao, O.; Nakai, H.; Klene, M.; Li, X.; Knox, J. E.; Hratchian, H. P.; Cross, J. B.; Bakken, V.; Adamo, C.; Jaramillo, J.; Gomperts, R.; Stratmann, R. E.; Yazyev, O.; Austin, A. J.; Cammi, R.; Pomelli, C.; Ochterski, J. W.; Ayala, P. Y.; Morokuma, K.; Voth, G. A.; Salvador, P.; Dannenberg, J. J.; Zakrzewski, V. G.; Dapprich, S.; Daniels, A. D.; Strain, M. C.; Farkas, O.; Malick, D. K.; Rabuck, A. D.; Raghavachari, K.; Foresman, J. B.; Ortiz, J. V.; Cui, Q.; Baboul, A. G.; Clifford, S.; Cioslowski, J.; Stefanov, B. B.; Liu, G.; Liashenko, A.; Piskorz, P.; Komaromi, I.; Martin, R. L.; Fox, D. J.; Keith, T.; Al-Laham, M. A.; Peng, C. Y.; Nanayakkara, A.; Challacombe, M.; Gill, P. M. W.; Johnson, B.; Chen, W.; Wong, M. W.; Gonzalez, C.; Pople, J. A. *Gaussian 03*, revision B.04; Gaussian, Inc.: Wallingford, CT, 2004.
(20) Becke, A. D. *J. Chem. Phys.* **1993**, *98*, 5648.
(21) Lee, C.; Yang, W.; Parr, R. G. *Phys. Rev. B* **1988**, *37*, 785. (b) Miehlich, B.; Savin, A.; Stoll, H.; Preuss, H. *Chem. Phys. Lett.* **1989**, *157*, 200.
(22) Dewar, M. J. S.; Thiel, W. *J. Am. Chem. Soc.* **1977**, *99*, 4899.
(23) Jovanovic, M. V.; Biehl, E. R. *J. Org. Chem.* **1984**, *49*, 1905.

Scheme 1

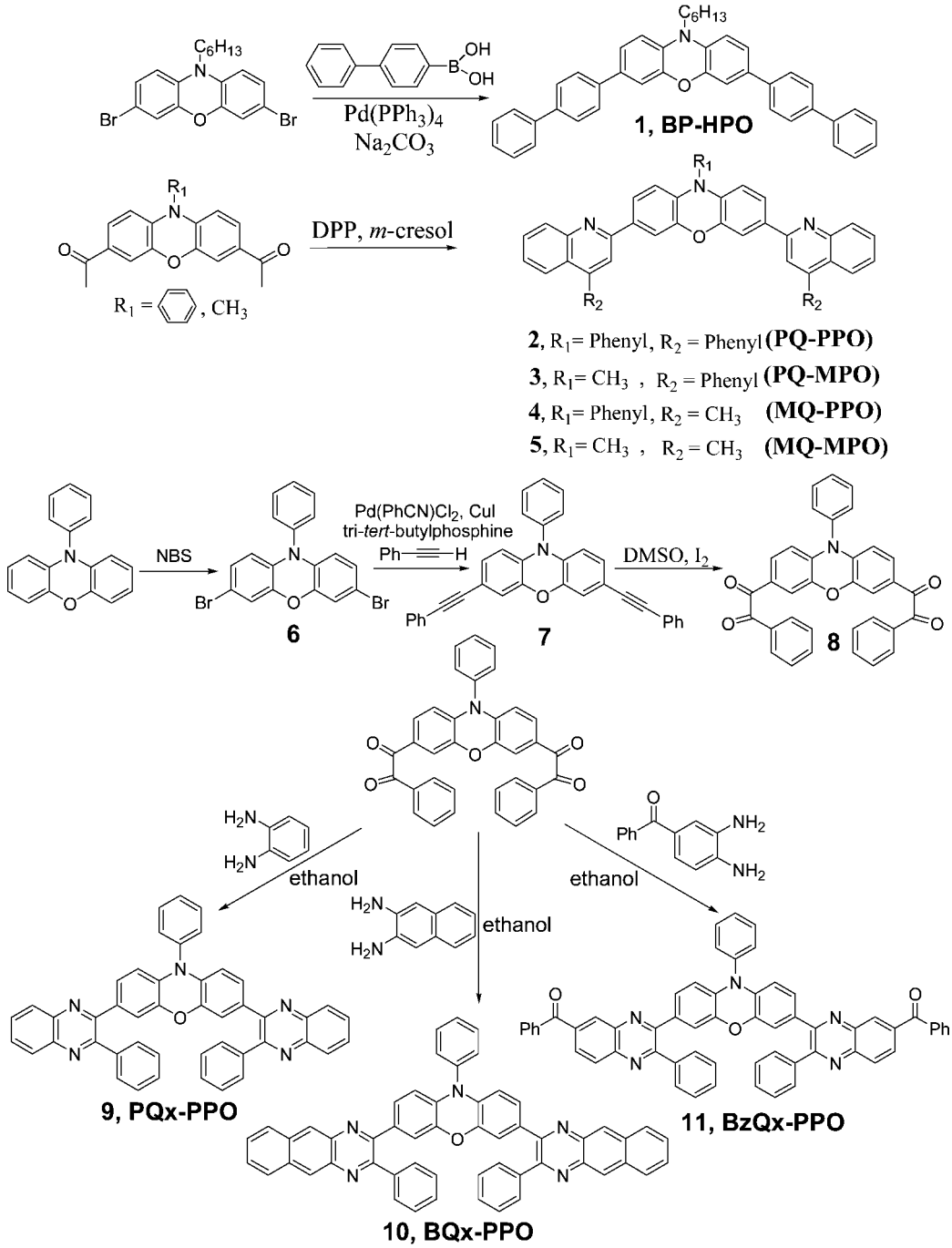

Table 1. Thermal and Photophysical Properties of Phenoxazine-Based D−A Molecules

compd	T_g/T_m[a] (°C)	T_d[b] (°C)	λ_{max}^{abs}[c] (nm)	λ_{max}^{em}[d] (nm)	fwhm[e] (nm)	ϕ_f(soln)[f]
BP-HPO, **1**	n.o./276	375	395	448	48	0.86
PQ-PPO, **2**	149/n.o.	484	430	474	47	0.81
PQ-MPO, **3**	137/311	442	430	487	48	0.74
MQ-PPO, **4**	128/312	421	426	477	47	0.77
MQ-MPO, **5**	n.o./311	406	425	477	47	0.77
PQx-PPO, **9**	154/n.o.	446	440	514	71	0.52
BQx-PPO, **10**	193/n.o.	473	476	564	80	0.16
BzQx-PPO, **11**	164/n.o.	501	468	560	85	0.41

[a] Glass transition temperature and melting temperature. n.o. = not observed. [b] Onset decomposition temperature. [c] Lowest energy absorption maximum in a dilute toluene solution. [d] PL emission maximum in a dilute toluene solution. [e] Full width at half-maximum of the PL emission spectrum in a toluene solution. [f] PL quantum yield in a dilute toluene solution.

structures were grown by slow evaporation of benzene or THF solutions. Both molecules were obtained as yellow plates or prisms, which provided excellent quality crystal data. PQ-PPO was found to cocrystallize with 1 equiv of benzene and to have a *c*-centered monoclinic C lattice with unit cell parameters of $a = 27.3440(10)$ Å, $b = 9.7620(3)$

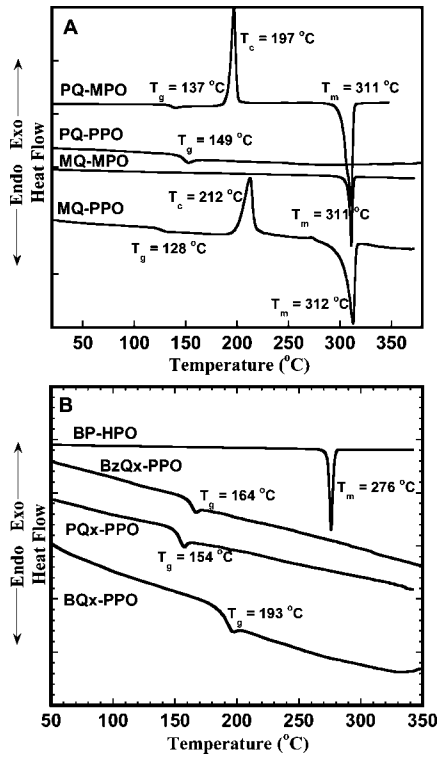

Figure 1. Second-heating DSC scans of phenoxazine-based D−A molecules.

Table 2. Crystallographic Data for PQ-PPO (2) and PQ-MPO (3)

	2	3
empirical formula	$C_{54}H_{37}N_3O$	$C_{51}H_{45}N_3O_3$
fw	743.87	747.90
cryst syst	monoclinic	monoclinic
cryst description/color	plate/yellow	prism/yellow
space group	*C*2/*c*	$P2_1/c$
a (Å)	27.3440(10)	17.5300(10)
b (Å)	9.7620(3)	8.1310(5)
c (Å)	30.2730(11)	30.8010(19)
β (deg)	94.2270(18)	119.927(2)
vol (Å^3)	8058.9(5)	3804.9(4)
temp (K)	130	130
Z	8	4
R_f	0.0562	0.0781
R_w	0.1142	0.1958
GOF	0.938	0.998

Å, c = 30.2730(11) Å, and β = 94.2270(18)°; the space group was *C*2/*c*. PQ-MPO cocrystallized with 1 equiv of THF in a primitive monoclinic crystal system with a = 17.5300(10) Å, b = 8.1310(5) Å, c = 30.8010(19) Å, and β = 119.927(2)°; the space group was $P2_1/c$. Both molecules are centrosymmetric with a point group symmetry of 2/*m* (C_h) as indicated by the space group symbols. The structures were refined to final residuals of R_1 = 5.62% for PQ-PPO and R_1 = 7.81% for PQ-MPO. The detailed crystallographic data for both molecules are collected in Table 2.

ORTEP diagrams of the single-crystal structures of PQ-PPO and PQ-MPO are shown in Figure 2. The tricyclic ring of the phenoxazine moiety in PQ-PPO and PQ-MPO is folded about the N−O axis with a dihedral angle of 169° between the two planes containing the benzene rings (C1−C6 and C16−C20). This dihedral angle (169°) shows that phenoxazine has a more planar conformation compared to its phenothiazine analogue, which has a dihedral angle of

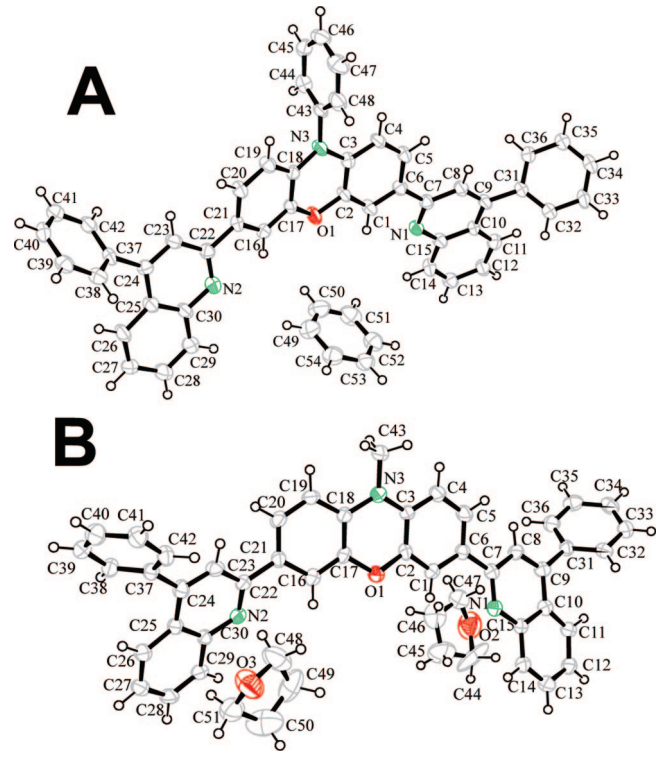

Figure 2. ORTEP diagrams of (A) PQ-PPO (**2**) and (B) PQ-MPO (**3**). Thermal ellipsoids are shown at their 50% probability volume. Solvent molecules, benzene and THF, that fill voids in the unit cells were found.

158.5° between the two benzene planes along the N−S axis.[24] A dihedral angle of 145° has been reported for a phenoxazine derivative, 2-methyl-2-phenoxazin-10-ylpropionitrile, which differs from our results.[25] The pendant 10-phenyl group in PQ-PPO is twisted 87° from the tricycle plane of the phenoxazine unit. The two quinoline moieties of PQ-PPO are distorted at angles of 15° and 19° relative to the neighboring benzene rings in the phenoxazine moiety, whereas the two quinoline moieties of PQ-MPO have torsion angles of 26° and 17° with respect to the phenoxazine plane. The 4-phenyl groups appended onto the quinoline moieties in PQ-PPO are twisted 54° and 57° relative to the quinoline moieties compared to 49° and 51° in PQ-MPO.

Figure 3 shows the packing diagrams of PQ-PPO and PQ-MPO. Two molecules of PQ-PPO related by inversion symmetry build a pair consisting of opposite dipole moments which cancels out the net dipole moment as shown in Figure 3A,i. Similar pairs were observed in PQ-MPO. Different pairs in both molecules are held together by van der Waals forces. The phenoxazine moieties in both molecules exhibit a face-to-face π-stacking with an intermolecular distance of 2.8 Å in PQ-PPO and 3.9 Å in MQ-PPO, whereas the quinoline moieties are too far apart to exhibit a clear π-stacking characteristic in both PQ-PPO and MQ-PPO. The solvent (benzene) molecule in PQ-PPO is positioned along the N−O axis of the phenoxazine moiety and exhibits a $\pi-\sigma$ stacking to the closest phenoxazine unit of one molecule and to the quinoline unit of another molecule. There is strong attractive interaction between oxygen atoms of the two THF solvent

(24) Pan, D.; Phillips, D. L. *J. Phys. Chem. A* **1999**, *103*, 4737.
(25) Gigmes, D.; Siri, D.; Reboul, J.-P.; Redouane, N.; Tordo, P.; Pèpe, G. *Acta Crystallogr.* **1998**, *C54*, 822.

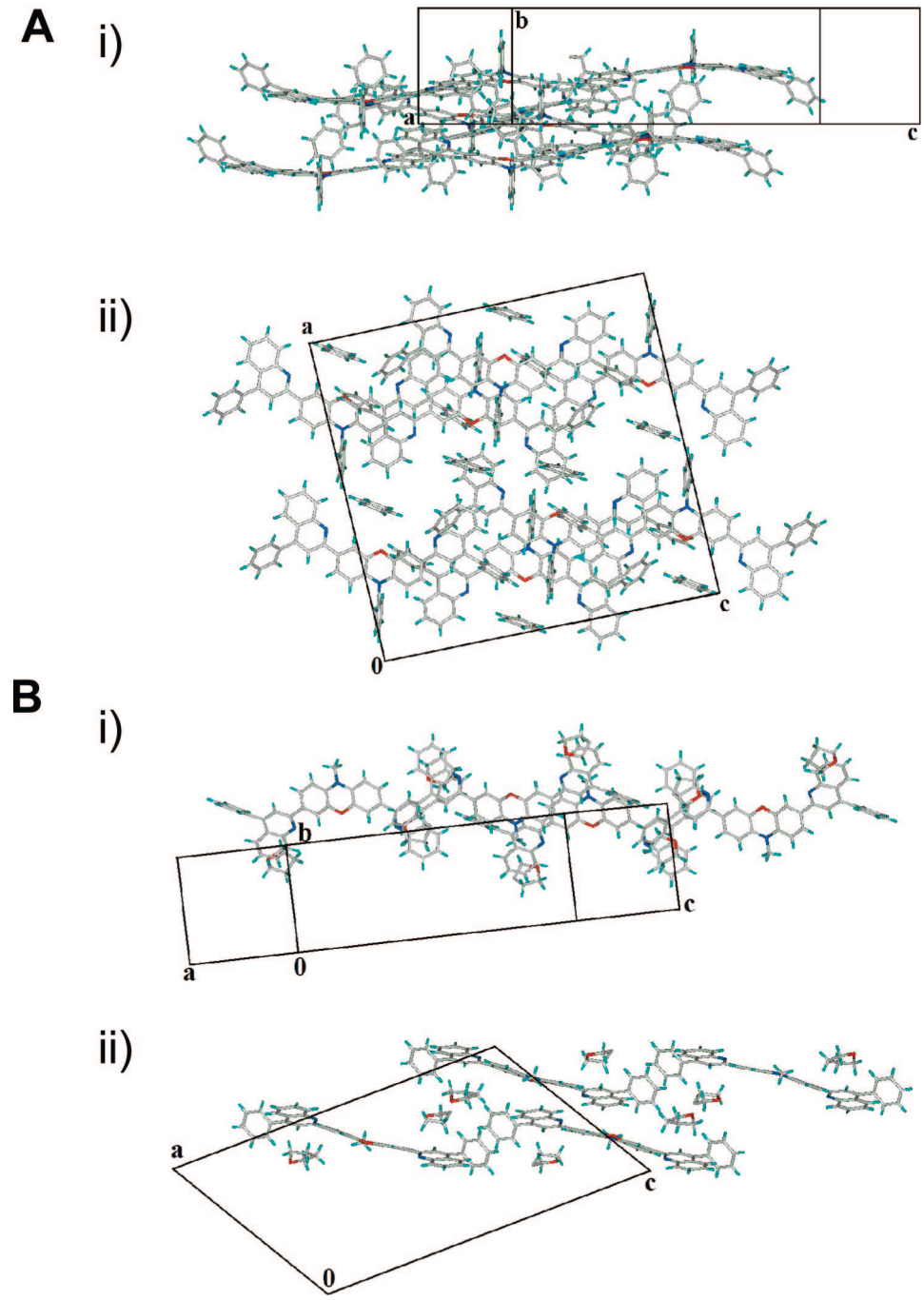

Figure 3. Packing diagrams of (A) PQ-PPO and (B) PQ-MPO: (i) view approximately normal to (100) and (ii) view normal to (010).

molecules in the PQ-MPO crystal and the nitrogen atoms of the quinoline moieties.

The single-crystal structures of PQ-PPO and PQ-MPO provide a basis for elucidating the effects of the solid-state morphology and molecular geometry on the photophysics, charge transport, and electronic properties of phenoxazine-based organic semiconductors being developed for organic electronics.

Electrochemical Properties. To understand the electronic structures of the phenoxazine D−A molecules with various electron acceptors, we performed cyclic voltammetry measurements on solutions of the molecules. Cyclic voltammograms (CVs) of all compounds in benzene/acetonitrile (2:1, v/v) are shown in Figure 4, and all the electrochemical data are summarized in Table 3. The oxidation and reduction waves of the four phenoxazine−quinoline D−A molecules in the scan range of −2.6 to +1.2 V (vs SCE) are shown in Figure 4A,B. A reversible oxidation wave and a quasireversible reduction wave were observed in the CV of each molecule. The CVs of the molecules can be repeatedly scanned many cycles in the range of −2.6 to +1.2 V (vs SCE) without a change in the redox characteristics. The half-wave oxidation ($E_{1/2}^{ox}$) and reduction ($E_{1/2}^{red}$) potentials of PQ-PPO are 0.79 and −2.00 V (vs SCE), respectively. Similar values were found for PQ-MPO, $E_{1/2}^{ox} = 0.71$ V and $E_{1/2}^{red} = -2.02$ V. The two 4-methylquinoline molecules MQ-PPO and MQ-MPO have identical half-wave oxidation and reduction potentials, 0.68 and −2.12 V, respectively.

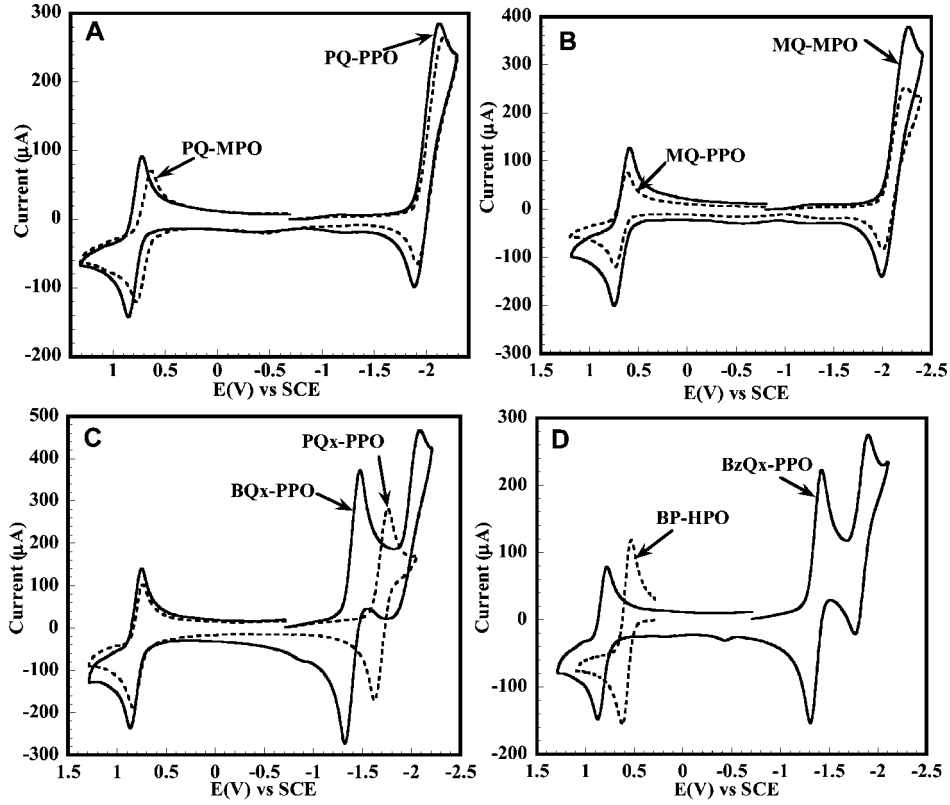

Figure 4. Cyclic voltammograms of a 1 mM solution of compounds **1**−**5** and **9**−**11** in benzene/acetonitrile (2:1, v/v) at a Pt electrode (0.1 M $TBAPF_6$, scan rate 200 mV/s).

Table 3. Redox Properties of Phenoxazine-Based D−A Molecules

compd	$E_{1/2}^{ox}$ [a] (V)	IP[b] (eV)	$E_{1/2}^{red}$ [c] (V)	EA[d] (eV)	E_g^{el} (eV)
BP-HPO, **1**	0.59	5.0			
PQ-PPO, **2**	0.79	5.2	−2.00	2.4	2.8
PQ-MPO, **3**	0.71	5.1	−2.02	2.4	2.7
MQ-PPO, **4**	0.68	5.1	−2.12	2.3	2.8
MQ-MPO, **5**	0.68	5.1	−2.12	2.3	2.8
PQx-PPO, **9**	0.79	5.2	−1.69	2.7	2.5
BQx-PPO, **10**	0.81	5.2	−1.40	3.0	2.2
BzQx-PPO, **11**	0.81	5.2	−1.37	3.0	2.2

[a] Half-wave oxidation potential vs SCE. [b] The ionization potential was obtained based on IP = $E_{1/2}^{ox}$ + 4.4 eV. [c] Half-wave reduction potential vs SCE. [d] EA = $E_{1/2}^{red}$ + 4.4 eV.

The observed $E_{1/2}^{ox}$ and $E_{1/2}^{red}$ of phenoxazine−quinoline molecules are very close to the half-wave redox potentials reported for 10-methylphenoxazine ($E_{1/2}^{ox}$ = 0.65 V vs SCE)[26] and 2-phenylquinoline ($E_{1/2}^{red}$ = −1.99 V vs SCE).[10d] This suggests that the oxidation and reduction waves in these molecules correspond to the formation of the phenoxazine radical cation and the quinoline radical anion, respectively. The close match of the redox potentials of phenoxazine−quinoline molecules to those of the parent D and A building blocks phenoxazine and quinoline suggests selective oxidation of phenoxazine and reduction of quinoline subunits in each D−A molecule. Similar results were previously observed in phenothiazine−phenylquinoline D−A molecules.[2c,d] This also implies localization of the HOMO and LUMO on the phenoxazine and quinoline moieties, respectively, in the D−A molecules and weak intramolecular D/A coupling in the ground state. From the observed half-wave potentials, we estimated ionization potential (IP) and electron affinity (EA) values, respectively, of 5.1−5.2 and 2.3−2.4 eV for the phenoxazine−quinoline molecules **2**−**5** by taking the SCE energy level to be −4.4 eV below the vacuum level (IP = $E_{1/2}^{ox}$ + 4.4, EA = $E_{1/2}^{red}$ + 4.4).[2b–e,27]

BP-HPO has a reversible oxidation wave with a half-wave oxidation potential of 0.59 V from which we estimated an IP of 5.0 eV for this molecule (Figure 4D). It did not show a reduction wave in the range from 0 to −3.0 V vs SCE since phenoxazine is a strong electron donor and the biphenyl group is an almost neutral moiety. CVs of the three phenoxazine−quinoxaline D−A molecules **9**−**11** are shown in Figure 4C,D. All three D−A molecules clearly show good reversibility of both oxidation and reduction waves as evident from the areas and close proximity of the anodic and cathodic peaks. Compounds **9**−**11** have a reversible oxidation wave with half-wave oxidation potentials of 0.79−0.81 V vs SCE, which are close to those of the other phenoxazine molecules **1**−**5** (Table 3). This indicates that the HOMOs of the phenoxazine−quinoxaline D−A molecules also lie on the phenoxazine moiety. The estimated ionization potentials of **9**−**11** are essentially identical, 5.2 eV.

As shown in Figure 4C,D, PQx-PPO has one reversible reduction wave whereas BQx-PPO and BzQx-PPO exhibit two reversible reduction waves. The half-wave reduction potentials of **9**−**11** vary from −1.69 V (vs SCE) for PQx-PPO to −1.37 V for BzQx-PPO. These values are significantly more positive than those of the phenoxazine−quinoline

(26) Spreitzer, H.; Scholz, M.; Gescheidt, G.; Daub, J. *Liebigs Ann.* **1996**, 2069. An $E_{1/2}^{ox}$ for 10-methylphenoxazine of 0.23 V vs F_c/F_c^+ was reported; we converted it to 0.65 V vs SCE by taking $E°(F_c/F_c^+)$ = 0.424 V vs SCE.[10d]

(27) Agrawal, A. K.; Jenekhe, S. A. *Chem. Mater.* **1996**, *8*, 579.

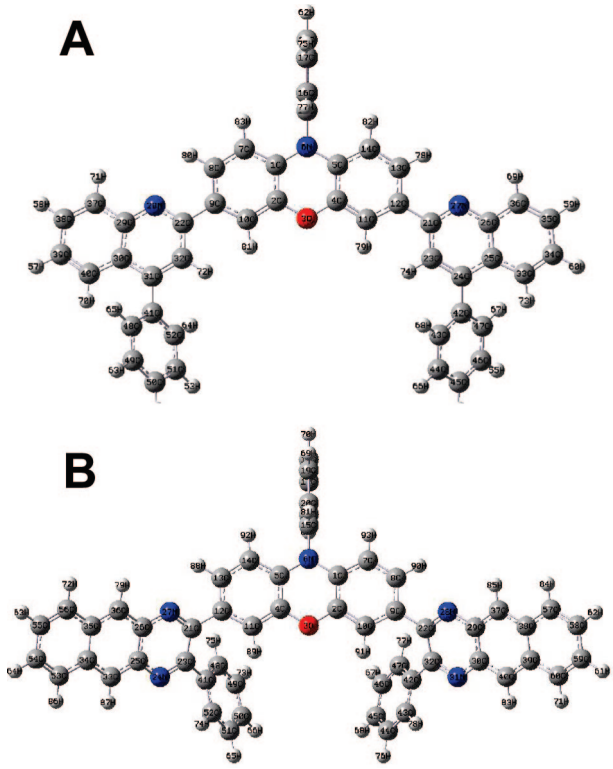

Figure 5. Optimized ground-state geometries of PQ-PPO (A) and BQx-PPO (B) predicted by DFT calculations.

D−A molecules (−2.12 to −2.00 V). It is obvious that the half-wave reduction potential is shifted to more positive values with increasing electron acceptor strength, as one goes from quinoline to quinoxaline to benzoquinoxaline or the benzoyl-substituted quinoxaline moiety in the D−A molecules. As a result, the estimated electron affinities of these D−A molecules increased from ∼2.4 eV in phenoxazine−quinoline molecules to 2.7 eV in PQx-PPO and 3.0 eV in BQx-PPO or BzQx-PPO (Table 3). The electrochemically derived HOMO−LUMO or band gaps (E_g^{el}) vary from 2.8 eV for phenoxazine−quinoline molecules **2**−**5** to 2.2 eV for BQx-PPO and BzQx-PPO. The highly reversible electrochemical oxidation and reduction of the phenoxazine D−A molecules suggest good prospects for efficient electron/hole injection and transport in organic electronic devices, especially organic light-emitting diodes. These results demonstrate that the electronic structures (HOMO/LUMO levels) and thus the electronic and optoelectronic properties of the donor−acceptor molecules can be readily manipulated by a judicious choice of the donor/acceptor units.

Quantum-Chemical Calculation of the Electronic Structure. DFT calculations were utilized to investigate the molecular geometry and electronic structures of the phenoxazine-based D−A molecules, compounds **2**, **4**, **5**, **9**, **10**, and **11**. Figure 5 shows the optimized ground-state geometries of two representatives of the D−A molecules, PQ-PPO and BQx-PPO, obtained with the B3LYP/6-31G* basis set. The electron donor moiety phenylphenoxazine (PPO) of both molecules exhibits fairly good planarity in its tricyclic structure with a dihedral angle (C7−C1−C2−O3 and O3−C4−C5−C14) of 179.5°, which is 10° higher than the 169° dihedral angle of the two benzene planes along the N−O axis determined by X-ray crystallography. The torsion angle between the phenoxazine donor and electron acceptor moiety determines the extent of coplanarity and electronic coupling between the D and A subunits in the D−A molecule. In the optimized PQ-PPO geometry as shown in Figure 5A, the torsion angle is described as C11−C12−C21−C23, which is found to be 13.06°. Thus, the two quinoline moieties of PQ-PPO are predicted to have a torsion angle of ∼13° relative to the neighboring benzene groups in the phenoxazine unit, which is comparable to the torsion angles (15−19°) determined by the X-ray single-crystal structure of PQ-PPO. In BQx-PPO, the torsion angle C10−C9−C22−C32 is 38.11°. The ∼25° smaller torsion angle in PQ-PPO suggests higher coplanarity between the acceptor and donor subunits in PQ-PPO compared to that in BQx-PPO. This can be explained by the stronger steric effect of the 3-phenyl groups in benzoquinoxaline (BQx) moieties than that of the 4-phenyl groups in phenylquinoline (PQ) moieties. MQ-PPO and MQ-MPO have torsion angles of 12.34° and 14.64° between methylquinoline and phenoxazine units, respectively, which are similar to that of PQ-PPO. Large torsion angles between the D and A subunits are found in PQx-PPO (38.54°) and BzQx-PPO (38.33°) due to the strong steric hindrance. In summary, the strong steric hindrance in PQx-PPO, BQx-PPO, and BzQx-PPO resulting from the 3-phenyl groups on their acceptor units leads to greater torsion angles and less coplanarity between the D and A moieties compared to those in the phenoxazine−quinoline molecules PQ-PPO, MQ-PPO, and MQ-MPO.

Figure 6 shows the plots of the molecular orbitals in the ground states of PQ-PPO and BQx-PPO. In PQ-PPO and BQx-PPO, the HOMOs and LUMOs are highly localized on the donor PPO and acceptor PQ/BQx moieties, respectively. However, the localization of the HOMOs is stronger than the localization of the LUMOs; the LUMOs extend beyond the acceptor PQ/BQx moieties to the adjacent phenoxazine unit. The LUMO energy level of BQx-PPO shows stronger localization on the acceptor BQx moieties compared to that in PQ-PPO since benzoquinoxaline is a stronger electron acceptor than phenylquinoline. The localization of HOMO/LUMO orbitals on donor/acceptor moieties has been commonly observed in previous theoretical studies on D−A molecules, indicating the occurrence of significant charge transfer in the HOMO → LUMO absorption transition.[28]

The calculated HOMO/LUMO energy levels and HOMO−LUMO gaps of six D−A molecules and their parent building blocks are listed in Table 4. Similar HOMO levels (−4.84 to −4.61 eV) were obtained for the D−A compounds **2**, **4**, **5**, **9**, **10**, and **11**, which are all close to the HOMO level of the PPO moiety (−4.61 eV). The calculated HOMO levels underestimate the experimental values obtained from cyclic voltammetry (∼−5.2 eV) by 0.3−0.5 eV. The calculated LUMO levels of the D−A molecules decrease with increas-

(28) (a) Elangovan, A.; Kao, K.-M.; Yang, S.-W.; Chen, Y.-L.; Ho, T.-I.; Su, Y. O. *J. Org. Chem.* **2005**, *70*, 4460. (b) Marsden, J. A.; Miller, J. J.; Shirtcliff, L. D.; Haley, M. M. *J. Am. Chem. Soc.* **2005**, *127*, 2464. (c) Ponce Ortiz, R.; Malavé Osuna, R.; Ruiz Delgado, M. C.; Casado, J.; Jenekhe, S. A.; Hernadez, V.; Lopez Navarrete, J. T. *Int. J. Quantum Chem.* **2005**, *104*, 635.

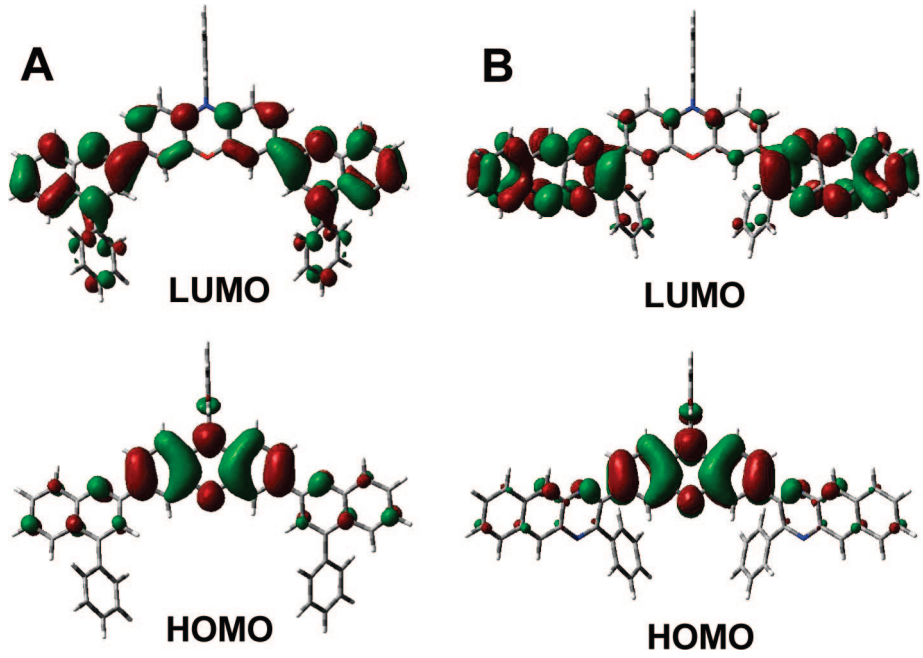

Figure 6. HOMO and LUMO orbitals of PQ-PPO (A) and BQx-PPO (B) in their optimized ground-state structures.

Table 4. Calculated HOMO/LUMO Energy Levels, Band Gaps, and Torsion Angles of Several D−A Compounds and Their Corresponding Donor and Acceptor Moieties[a]

compd	HOMO (eV)	LUMO (eV)	band gap (eV)	torsion angle (deg)
PQ-PPO, **2**	−4.62	−1.60	3.02	13.06
MQ-PPO, **4**	−4.61	−1.52	3.09	12.34
MQ-MPO, **5**	−4.71	−1.53	3.18	14.64
PQx-PPO, **9**	−4.75	−1.85	2.90	38.54
BQx-PPO, **10**	−4.75	−2.20	2.55	38.11
BzQx-PPO, **11**	−4.84	−2.24	2.60	38.33
PPO	−4.61	−0.49	4.12	
PQ	−6.10	−1.47	4.63	
PQx	−6.26	−1.98	4.28	
BQx	−5.66	−2.30	3.36	
BzQx	−6.42	−2.36	4.06	

[a] DFT//B3LYP/6-31G*.

ing strength of the electron acceptors, varing from −1.52 eV for MQ-PPO to −2.24 eV for BzQx-PPO. The theoretically predicted LUMO levels are about ∼0.8 eV higher lying than those estimated experimentally. It has been found previously that the predicted LUMO energy levels of heteroaromatic molecules underestimate the cyclic voltammetry derived values by 0.6−0.8 eV.[29] The calculated LUMO levels of the D−A molecules match well with the LUMO levels of their parent acceptor building blocks (Table 4). The predicted HOMO−LUMO gaps of the D−A molecules (2.55−3.18 eV) are 0.2−0.4 eV higher than experimentally estimated electrochemical band gaps (E_g^{el} = 2.2−2.8 eV). This is mainly due to the underestimation of the LUMO levels. Overall, the initial DFT calculations on the D−A molecules predict well the experimentally observed trends in the redox properties and provide insights into their electronic structures in the ground state.

Photophysical Properties. Figure 7a shows the normalized optical absorption spectra of the eight D−A molecules

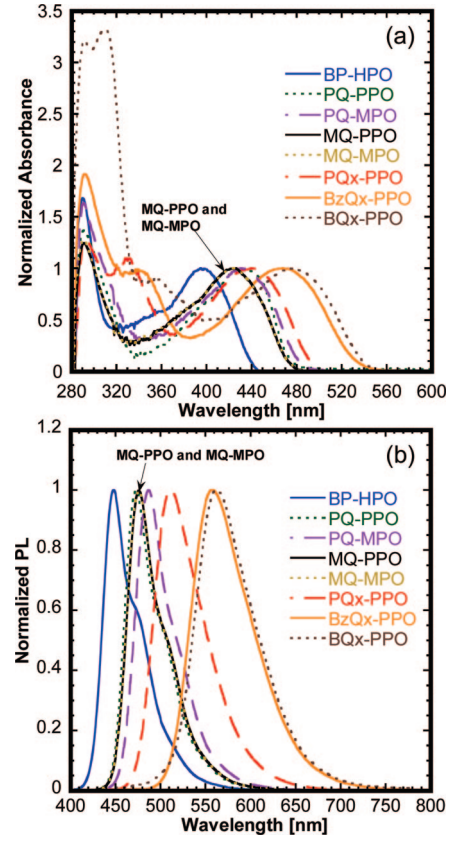

Figure 7. Normalized optical absorption spectra (a) and normalized PL emission spectra (b) of the donor−acceptor molecules in a dilute (2−5 × 10^{-6} M) toluene solution. The excitation wavelength used was 415 nm in all cases, except BP-HPO, where it was 380 nm.

in a dilute (2−5 × 10^{-6} M) toluene solution. Two prominent absorption features were observed in the spectra of all the D−A molecules: a lower intensity band in the 395−475 nm range and a higher intensity band in the 290−295 nm range along with additional peaks in the 310−360 nm range in some molecules. In all molecules, the high-energy peaks have

(29) Zhu, Y.; Yen, C. T.; Jenekhe, S. A.; Chen, W. C. *Macromol. Rapid Commun.* **2004**, *25*, 1829.

larger extinction coefficients (ε) compared to that of the lowest-energy peak. The high-energy absorption bands are associated with the $\pi-\pi^*$ transitions of the D−A molecules, localized on either the D or A moiety of the molecule. The lowest energy absorption band observed in all the molecules is completely absent in the absorption spectra of the parent D and A building blocks. Therefore, the lowest energy absorption band can be assigned to the ICT transition ^{1}CT ← S_0 in each D−A molecule.[2a–e] As the strength of the electron acceptor increases, the ICT absorption band of the D−A molecule gradually red shifts. For example, the ICT absorption maximum red shifts from 430 nm in PQ-PPO to 440 nm in PQx-PPO to 476 nm in BQx-PPO as the electron acceptor moiety goes from quinoline to quinoxaline to benzoquinoxaline, respectively. Given that the electron donor moiety in all the molecules is the same, the observed red shift can be understood to arise from the larger ground-state dipole moments and the larger ICT effects with increasing electron acceptor strength. The absorption onset correspondingly red shifts from ~475 nm in MQ-MPO to ~500 nm in PQx-PPO to ~540 nm in BQx-PPO, indicating a reduction in the optical band gap of the D−A molecule with increasing electron-accepting strength of A. The absorption onsets and peak maxima of BzQx-PPO and BQx-PPO are very similar, suggesting similar electron-accepting strength of benzoylquinoxaline and benzoquinoxaline moieties. The four molecules containing quinoline acceptors have very similar absorption characteristics; in fact, MQ-PPO and MQ-MPO show identical absorption bands as indicated in Figure 7a. The methyl and phenyl substitutions on the quinoline and phenoxazine moieties apparently have little or no effect on the ground-state electronic structure of the phenoxazine−quinoline D−A molecules. The photophysical properties of the D−A molecules are summarized in Table 1.

Figure 7b shows the normalized PL emission spectra of the D−A molecules in a dilute ($2-5 \times 10^{-6}$ M) toluene solution. The emission spectra of the D−A molecules dramatically red shift with increasing electron-accepting strength. BP-HPO emits a blue color in solution with a maximum at 448 nm and a full width at half-maximum (fwhm) of 48 nm. The four quinoline-containing molecules have blue-green emission with PL maxima in the 477−487 nm range. PQx-PPO with a quinoxaline acceptor emits a green color in solution (fwhm = 71 nm). Orange-red emission is observed from both BzQx-PPO and BQx-PPO with similar PL maxima (560−564 nm) and fwhm values (80−85 nm). The obvious reason for the observed red shift is the greater degree of ICT (increasing excited-state dipole moments) with increasing electron acceptor strength in going from quinoline to quinoxaline to benzoquinoxaline (or benzoylquinoxaline). Thus, emission colors spanning the entire visible region are obtained from the phenoxazine-based D−A molecules, demonstrating how charge transfer and the resultant ICT fluorescence in a D−A molecule can be effectively manipulated through the electron-accepting strength of the acceptor building block.

Additional evidence supporting the stronger ICT effects with increasing strength of the electron acceptor in the D−A molecules comes from their PL quantum yields (ϕ_f) in toluene solutions. It is well-known that the ϕ_f value of a D−A molecule decreases with increasing excited-state ICT interaction.[2a–e] We found that the ϕ_f values of these D−A molecules steadily decreased with increasing strength of the acceptor block (Table 1). High ϕ_f values of 0.86 and 0.74−0.81 were obtained for BP-HPO and the four phenoxazine-quinoline molecules. The values gradually decreased from 0.52 in PQx-PPO to 0.41 in BzQx-PPO to as low as 0.16 in BQx-PPO. The much lower ϕ_f value of BQx-PPO relative to BzQx-PPO likely suggests greater degree of ICT in the excited state of the former. Thus, the lowest value is obtained in BQx-PPO, which is to be expected from its absorption spectrum (Figure 7a). Among all the D−A molecules, the intensity (oscillator strength) of the ^{1}CT ← S_0 transition relative to the $\pi-\pi^*$ transition was the lowest in BQx-PPO. On the basis of this fact and Einstein's relationship, which relates the absorption coefficient and the rate constant of spontaneous emission,[30] the lowest ϕ_f value is to be expected in BQx-PPO.

Conclusions

We have synthesized a series of new phenoxazine-based donor−acceptor molecules and investigated their crystal structures and thermal, electrochemical, and photophysical properties. Single-crystal X-ray structures of PQ-PPO and PQ-MPO showed that they crystallized in the monoclinic system with the space groups $C2/c$ and $P2_1/c$, respectively. A dihedral angle of 169° between the two phenyl planes along the N−O axis was found in the phenoxazine moieties of both molecules. The D−A molecules exhibited intramolecular charge transfer fluorescence with a PL quantum yield from 77−81% in phenoxazine−quinoline molecules to as low as 16% in the phenoxazine−benzoquinoxaline molecule. The D−A molecules possess high glass transition temperatures (128−193 °C). They exhibit highly reversible electrochemical oxidation and reduction, indicating ambipolar redox properties that could facilitate efficient hole/electron injection, transport, and charge recombination. The phenoxazine-based D−A molecules have low ionization potentials (5.0−5.2 eV), while their electron affinities were increased from ~2.4 eV in the quinoline-containing molecules to 3.0 eV in BQx-PPO and BzQx-PPO. The DFT calculations were in good agreement with the experimental results in predicting the molecular geometry and electronic structures of the D−A molecules. These results demonstrate that phenoxazine is an excellent electron donor building block for the design of new emissive and charge transport materials for OLEDs and other organic electronics. The thin film properties and application of the materials in OLEDs and thin film transistors will be reported separately.[31]

Acknowledgment. This research was supported by the NSF (Grant CTS-0437912), Air Force Office of Scientific Research EHSS MURI (Grant F9550-06-1-0326), and NSF STC MDITR (Grant DMR-0120967). We thank Professor Werner Kaminsky for the X-ray single-crystal structures.

CM702212W

(30) Pope, M.; Swenberg, C. E. *Electronic Processes in Organic Crystals*; Oxford University Press: New York, 1999; Chapter I.

(31) Part 2 in the series: Kulkarni, A. P.; Zhu, Y.; Babel, A.; Wu, P.-T.; Jenekhe, S. A. *Chem. Mater.* **2008**, *20*, 4212–4223.